C. elegans sperm bud vesicles to deliver a meiotic maturation signal to distant oocytes

Mary Kosinski[1], Kent McDonald[2], Joel Schwartz[3], Ikuko Yamamoto[1] and David Greenstein[1,*]

[1]Department of Cell and Developmental Biology, Vanderbilt University School of Medicine, 465 21st Avenue South, Nashville, TN 37232, USA
[2]Electron Microscopy Laboratory, University of California, Berkeley, 26 Giannini Hall, Berkeley, CA 94720-3330, USA
[3]Department of Molecular Physiology and Biophysics, Vanderbilt University School of Medicine, 465 21st Avenue South, Nashville, TN 37232, USA
*Author for correspondence (e-mail: david.greenstein@vanderbilt.edu)

Accepted 23 May 2005

Development 132, 3357-3369
Published by The Company of Biologists 2005
doi:10.1242/dev.01916

Summary

The major sperm protein (MSP) is the central cytoskeletal element required for actin-independent motility of nematode spermatozoa. MSP has a dual role in *Caenorhabditis elegans* reproduction, functioning as a hormone for both oocyte meiotic maturation and ovarian muscle contraction. The identification of the signaling function of MSP raised the question, how do spermatozoa, which are devoid of ribosomes, ER and Golgi, release a cytoplasmic protein lacking a signal sequence? Here, we provide evidence that MSP export occurs by the budding of novel vesicles that have both inner and outer membranes with MSP sandwiched in between. MSP vesicles are apparently labile structures that generate long-range MSP gradients for signaling at the oocyte cell surface. Both spermatozoa and non-motile spermatids bud MSP vesicles, but their stability and signaling properties differ. Budding protrusions from the cell body contain MSP, but not the MSD proteins, which counteract MSP filament assembly. We propose that MSP generates the protrusive force for its own vesicular export.

Key words: Oogenesis, Meiotic maturation, Gamete interactions, Major sperm protein signaling, Vesicle budding, Unconventional protein secretion

Introduction

Intercellular communication between sperm and oocyte is fundamental for sexual reproduction (Hardy, 2002). Long- and short-range signaling mechanisms control a medley of essential reproductive processes, including sperm chemotaxis, oocyte meiotic maturation, gamete recognition, cell fusion and egg activation. Studies of diverse organisms reveal striking cell biological parallels in the molecular underpinnings of gametic interactions. Many marine invertebrates broadcast sperm into the sea, which then depend on long-range chemotactic cues to locate and fertilize eggs (Ward et al., 1985). Sperm chemotaxis also occurs in the mammalian female reproductive tract (Eisenbach and Tur-Kaspa, 1999) and may involve the function of conserved olfactory receptors (Spehr et al., 2003). Egg surface components, such as the ZP3 glycoprotein in mammals and the fucose sulfate polymer in sea urchins, mediate short-range signaling that induces the acrosome reaction, a highly specialized exocytic event needed for zona penetration and gamete fusion (Wassarman et al., 2001; Neill and Vacquier, 2004).

In many animals, including many species of sponges, annelids, mollusks and nematodes, sperm promote the resumption of meiosis in arrested oocytes (Masui, 1985; McCarter et al., 1999). In *Caenorhabditis elegans*, sperm use the major sperm protein (MSP) as a hormone to promote oocyte meiotic maturation and gonadal sheath cell contraction at a distance (Miller et al., 2001). MSP is also the key cytoskeletal element required for amoeboid locomotion of nematode sperm (Italiano et al., 1996). MSP promotes oocyte meiotic maturation, in part by binding the VAB-1 Eph receptor protein-tyrosine kinase on oocytes, and by antagonizing an inhibitory somatic gonadal sheath cell pathway (Miller et al., 2003). *C. elegans* hermaphrodites reproduce by either self-fertilization or mating with males (Hubbard and Greenstein, 2000). Because a hermaphrodite produces only a fixed number of sperm, oocyte meiotic maturation occurs constitutively until sperm become limiting. In females lacking sperm, oocytes arrest in meiotic prophase until insemination. Thus, the MSP hormone functions as the linchpin of a sperm-sensing mechanism linking meiotic maturation and sperm availability. Proteins with MSP domains are widespread and five human genes encode proteins containing this domain. Recently, a mutation in the MSP domain of VAPB was shown to cause spinal muscular atrophy and amyotrophic lateral sclerosis type 8 (Nishimura et al., 2004). Studies of MSP signaling, motility, or release in *C. elegans* may thus provide information about the functions of this conserved domain.

MSP release probably occurs through an unconventional mechanism because sperm lack the cellular components required in standard models of protein secretion, such as ribosomes, endoplasmic reticulum (ER) and Golgi. Moreover, MSP was defined as a cytoplasmic protein lacking an N-terminal leader sequence, and there is no evidence for proteolytic processing (Klass and Hirsh, 1981; Miller et al., 2001). Here, we address the question of how sperm release

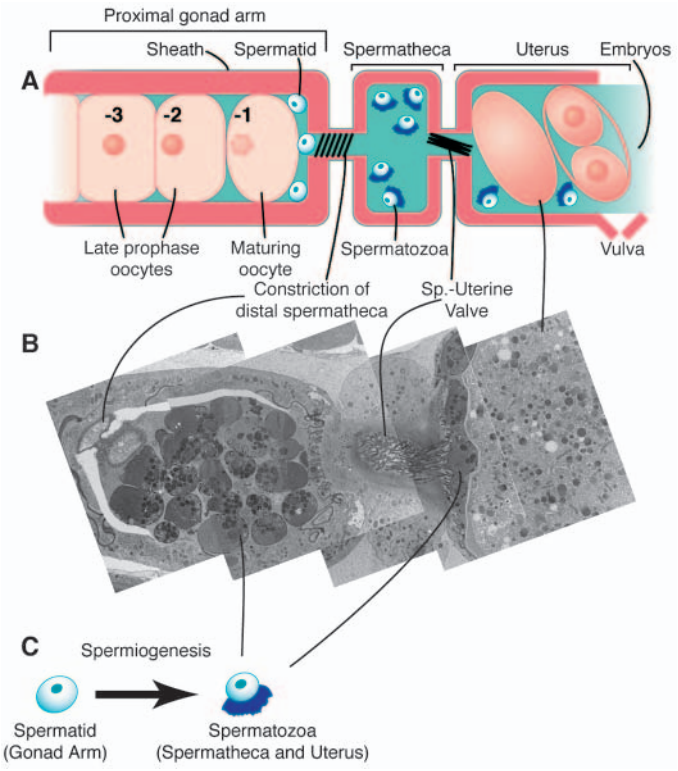

Fig. 1. Anatomy of MSP signaling. (A) Diagram of the hermaphrodite reproductive tract. Oocytes undergo meiotic maturation in an assembly line fashion in response to MSP signaling. At ovulation, the distal constriction of the spermatheca dilates, the oocyte enters and is fertilized. (B) Electron micrograph of the spermatheca. Spermatozoa are unable to enter the proximal gonad because the constriction of the distal spermatheca provides a barrier. Some spermatozoa enter the uterus with embryos, and must then crawl back into the spermatheca so they can fertilize oocytes. (C) Spermiogenesis is the process during which non-motile spermatids become fertilization-competent motile spermatozoa with a pseudopod. Spermiogenesis occurs when spermatids enter the spermatheca during the first ovulation in hermaphrodites, or as they enter the uterus during mating. In A, a few spermatids are shown remaining in the gonad arm, as is typically seen on the first two days of adulthood. These spermatids will enter the spermatheca in the next few ovulations.

MSP to signal oocytes and sheath cells at a distance in a complex reproductive tract (Fig. 1). We demonstrate that spermatids and spermatozoa release MSP by a novel vesicle-budding mechanism. Spermatids and spermatozoa differ in their signaling potencies. Spermatozoa produce a long-range signal that is temporally labile, whereas spermatids provide a long-acting, more local signal. We propose that differential vesicle stability determines the physical and temporal range of signaling.

Materials and methods

Nematode strains and phenotypic analysis

Standard techniques were used for nematode culture at 20°C. Wild-type nematode strains were: *C. elegans* N2, *C. briggsae* AF16, *C. remanei* PB206, *Poikilolaimus regenfussi* SB199, *Acrobeloides maximus* DF5048 (Thorne, 1925) and *Zeldia puncta* PDL0003 (De Ley et al., 1990). *C. elegans* females are genetically altered XX animals that produce no sperm. Mutations and rearrangements were (see l'Hernault et al., 1988; Riddle et al., 1997):

LGI, *spe-8(hc50)*;

LGIV, *spe-27(it110)*, *unc-24(e138)*, *fem-3(e1996)*, *nT1(IV, V)*; and

LGV, *emo-1(oz1)*, *fog-2(q71)*.

Oocyte meiotic maturations rates and MAPK activation were analyzed as described (Miller et al., 2001). Spermatozoa were labeled using 75 μM MitoTracker Red CMXRos (Molecular Probes) by modifying the method of Hill and L'Hernault (Hill and L'Hernault, 2001). *spe-8(hc50)* hermaphrodites were feminized using RNAi feeding of L1 larvae (Kamath et al., 2001).

Antibodies, western blotting and immunocytochemistry

Standard methods were used to raise, purify and characterize antibodies (Harlow and Lane, 1988). Peptides were purchased from Open Biosystems and purified by HPLC. Three fixation methods were used: (1) dissected gonads with 3% paraformaldehyde (Rose et al., 1997); (2) dissected gonads with methanol; or (3) wholemounts with Bouin's reagent (Nonet et al., 1997). Fourteen different antibody preparations were used to examine MSP localization. The only differences observed were the sensitivity of detection and the fixation methods required, as indicated below. Polyclonal antibodies were affinity-purified using peptides coupled to CNBr-activated sepharose (Amersham Biosciences) or SulfoLink resin (Pierce). For the purification of monoclonal antibodies, hybridomas were grown in serum-free medium and purified on protein A/G columns (Amersham Biosciences). The N-terminal-specific antibodies were raised to MSP (1-22) AQSVPPGDIQTQPGTKIVFNAP (2 rabbits, method 1). C-terminal-specific antibodies were raised to: MSP (107-126) EWFQGDMVRRKNLPIEYNP (2 rabbits, methods 1 and 2); and CGG-MSP (106-126) CGGREWFQGDMVRRKNLPIEYNP [2 rabbits, method 1; 5 mice, methods 1 and 3; and 2 monoclonal hybridomas, method 1 and electron microscopy using post-embedding immunohistochemistry (immunoEM)]. We also used mAbTR-20 raised to MSP (Ward et al., 1986) (methods 1 and 3, and immuno EM). Antibodies to MSD proteins were raised to CGG-MSD (53-73) CGGDPSGSKDITITRTAGAPKEDK (2 rabbits, methods 1 and 3). Other antibodies used were: RME-2 (Grant and Hirsh, 1999), and Cy2-, Cy3- or Cy5-conjugated secondary antibodies (Jackson ImmunoResearch Laboratories).

For western blotting, protein lysates were prepared from 10 staged adults, and analyzed by electrophoresis on 4-12% NuPage gels (Invitrogen). The signal was detected with SuperSignal West Femto reagent (Pierce). Blots were quantitated using a VersaDoc imager with QuantityOne software (Bio-Rad).

Fluorescence microscopy

Wide-field fluorescence microscopy employed Zeiss Axioskop or Axioplan microscopes using 63× and 100× (NA1.4) objective lenses. Images were acquired with an ORCA ER (Hamamatsu) charge-coupled device camera using OpenLab (Improvision) or MetaMorph (Universal Imaging) acquisition software. Pixel intensities were measured in arbitrary fluorescent units. All exposures were within the dynamic range of the detector. Measurements at 10 different points within areas of interest were averaged, and background levels subtracted as described (Miller et al., 2003). DNA was detected with DAPI.

Confocal images were acquired on a Zeiss LSM510 microscope using a pinhole of 1.42 Airy units and 63× and 100× (NA1.4) objective lenses. Gain and offset were set so that all data was within the dynamic range of the PMT. Band pass filters were used to optically isolate the Cy2, Cy3 and Cy5 fluorophores, and no cross-talk was observed. For the reconstructions shown in Fig. 3B,E, serial images were smoothed with a Gaussian filter, and an isosurface and voltex were constructed using Amira (Amiravis). The images were transferred to QuickTime format using VR Worx (VR Toolbox). DNA in some samples was detected with propidium iodide (Molecular Probes).

Electron microscopy

Samples were prepared for TEM by high-pressure freezing and freeze substitution (Howe et al., 2001; Müller-Reichert et al., 2003). Wild-type (*n*=2), *fog-2(q71)* (*n*=3), and *spe-8(hc50)* (*n*=3) animals were viewed in serial longitudinal sections. For immunoEM, wild-type (*n*=2) and *spe-8(hc50)* (*n*=2) samples were prepared according to Lonsdale et al. (Lonsdale et al., 1999), using 0.25% glutaraldehyde as a fixative. Thin-layer embedding in LR White (Ted Pella) was used so that tissue preservation could be assessed by light microscopy and the sample could be oriented for sectioning (Lonsdale et al., 2001). Longitudinal thin sections (70 nm) were placed on formvar-coated grids and stained with 5-10 μg/ml mAb4D5 anti-MSP. Secondary antibodies conjugated with 10 nm gold particles (Amersham Biosciences) were used for detection. Grids were examined using a Philips CM-12, 120 keV electron microscope at 80 kV. Mated (*n*=1) and unmated (*n*=1) *fog-2(q71)* female samples were also prepared for TEM and immunoEM by conventional methods (Hall et al., 1999). Immunolabeling of spermatozoa within mated females was comparable to that obtained by the HPF method, but extracellular spaces in the spermatheca were not well preserved, and MSP vesicles were not seen. No labeling was observed in unmated females.

Results

Release of MSP from spermatozoa

Previous studies reported the intracellular localization of MSP during spermatogenesis (Klass and Hirsh, 1981; Ward and Klass, 1982). To examine MSP release from spermatozoa, we raised a battery of polyclonal and monoclonal antibodies to N- and C-terminal MSP peptides. The antibodies detect an abundant ~15 kDa polypeptide, co-migrating with purified MSP, in western blots of total protein extracts from mated *fog-2(q71)* females and males, but not from unmated females or *E. coli* extracts (Fig. 2A, and data not shown).

To analyze MSP release from spermatozoa in vivo, we examined gonads of mated *fog-2(q71)* female animals using immunofluorescence (Fig. 2B,C). In mated females, spermatozoa are only observed in the spermatheca and uterus; however, we observed MSP extending past the distal constriction into the proximal gonad arm. This staining represents MSP that is extracellular to spermatozoa. By contrast, all unmated females showed no staining (Fig. 2B, right panel; *n*=51). Using anti-MSP mAbTR-20 and visual inspection, 91% of mated female gonad arms exhibited extracellular MSP localization (*n*=36), with 39% showing extracellular MSP as far as the most proximal (–1) oocyte, and the rest exhibiting extracellular MSP only within the spermatheca. Within the spermatheca, MSP staining was judged to be outside of spermatozoa if staining extended at least 5 μm beyond the pseudopod or cell body. MSP staining extended on average 33.6±19 μm (maximal range=90 μm; *n*=12) from spermatozoa, which are approximately 5 μm in size. When the spermatheca contained more than 50 spermatozoa, MSP extended to an average maximal distance of approximately 60 μm from spermatozoa (Fig. 2D). By contrast, when the spermatheca contained less than 50 spermatozoa, MSP extended to an average maximal distance of approximately 22 μm from spermatozoa (Fig. 2D). In adult hermaphrodites, we detected MSP outside of spermatozoa during days 1-3 of adulthood (see Fig. S1A-C in the supplementary material), but not at day 5, when no spermatozoa remain (see Fig. S1E). Thus, the distribution of extracellular MSP in the gonad correlates with sperm availability. Extracellular MSP was seen in mated *C. remanei* females, as well as in *C. briggsae* and *Poikilolaimus regenfussi* hermaphrodites (data not shown).

In mated females, extracellular MSP exhibits a graded distribution, with a sharp boundary between the –1 and –2 oocytes (Fig. 2B,C). Fluorescence intensity measurements indicate that MSP is localized in a graded manner from the spermatheca to the –1 oocyte (Fig. 2C, *n*=10). Fluorescence intensity measurements also indicate that there is significant MSP staining over the –2 and –3 oocytes (Fig. 2E). MSP binds the VAB-1 MSP/Eph receptor and unidentified receptors, which are expressed in the proximal gonad (Miller et al., 2003). One explanation for the sharp boundary in staining intensity between the –1 and –2 oocytes is that MSP receptors may act as a sink for MSP vectorially presented from the spermatheca. To test this hypothesis, we examined extracellular MSP localization in mated *emo-1/sec-61γ(oz1)* females, which are defective for secretion in the germ line (Iwasaki et al., 1996) and MSP binding to oocytes (Miller et al., 2003). Mated *emo-1(oz1)* females animals did not exhibit a sharp boundary between the most proximal two oocytes, and quantitative analysis showed no significant difference in staining intensity of the –1 to –3 oocytes (Fig. 2E). Instead, MSP extended further distally in mated *emo-1(oz1)* females, when compared with unmated controls, frequently reaching the loop region more than 100 μm away (data not shown). These results suggest that receptors may influence boundary formation by restricting diffusion.

Extracellular MSP is punctate and diffuse and localizes to the oocyte cell surface

With confocal microscopy, extracellular MSP appeared both punctate and diffuse in the spermatheca, the gonad arm and the uterus (Fig. 2F, see Movie 1 in the supplementary material). Analysis of 3D data stacks indicated that punctate extracellular MSP was enriched near spermatozoa on the spermathecal walls (Fig. 2F). The largest puncta were at the diffraction limit of our microscope (0.5 μm) and were found nearby spermatozoa. In the proximal gonad arm, MSP was more diffuse and localized in focal plane slices near the oocyte surface (Fig. 2F, Movie 1 in the supplementary material; see below for further confirmation). In the uterus, we observed large MSP puncta close to spermatozoa (Fig. 2F, right panel; see Movie 2 in the supplementary material). We also observed diffuse MSP in extracellular spaces surrounding embryos in the uterus (Fig. 2F, see Movie 2). We were able to visualize MSP puncta near spermatozoa in the uterus and spermatheca using wide-field microscopy, when these regions were less crowded with spermatozoa (Fig. 2G). These results are consistent with the possibility that the large MSP puncta arise from spermatozoa and generate a diffuse MSP signal in the proximal gonad.

To pinpoint the localization of MSP at the oocyte cell surface, we conducted a 3D confocal analysis of MSP localization in mated females using the RME-2 yolk receptor to mark the oocyte plasma membrane and the early endosomal compartments (Grant and Hirsh, 1999). Three-dimensional image reconstructions of the data indicate that MSP localizes in three regions: (1) in superficial focal planes at the oocyte cell surface with RME-2 just beneath; (2) in the same plane as the RME-2 signal; and (3) within the oocyte beneath the

plasma membrane (Fig. 3A,B, see also Movies 3, 4 in the supplementary material). These results are consistent with data showing that MSP is an extracellular signal that binds receptors on the oocyte surface, and suggest the MSP signal is endocytosed.

Specificity of MSP release and apparent budding from spermatozoa

Retrospective sperm counting experiments indicate that every spermatozoa fertilizes an oocyte (Ward and Carrel, 1979). Nonetheless, we used vital dye labeling with MitoTracker Red to address whether MSP release results from lysis, the expectation being that lysis would disrupt the structure and integrity of spermatozoa dispersing the label. To label spermatozoa, males were soaked in MitoTracker Red (Hill and L'Hernault, 2001) and mated to unlabeled females. Labeled spermatozoa were able to crawl to the spermatheca of unlabeled females and produce viable progeny. The labeled mitochondria were located in a tight cluster in the cell body surrounding the spermatozoa chromatin (Fig. 3C). By contrast,

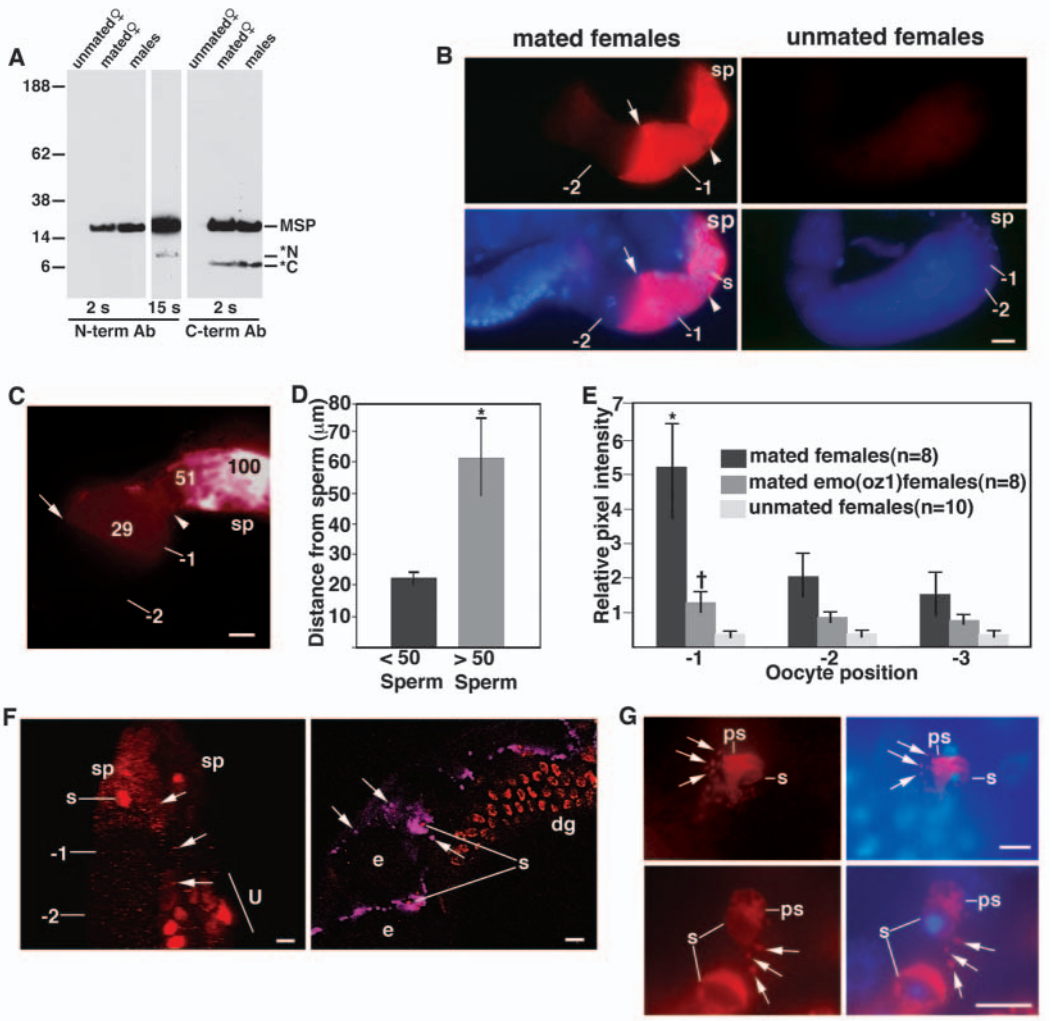

Fig. 2. Evidence that spermatozoa release MSP. (A) Western blot. Males and mated females contain MSP, but unmated females do not. Minor N- and C-terminal fragments (*N and *C) result from scission of MSP during the boiling step of lysate preparation (data not shown). The male lysate was overexposed to visualize *N (center lane, 15 seconds exposure time). (B,C) Detection of MSP (red) in the proximal gonad arm of mated females (left panels in B). MSP extends beyond the distal constriction (arrowhead) of the spermatheca (sp). A sharp boundary in staining intensity is observed between the –1 and –2 oocytes (arrow). DNA (blue) is shown in the merged images (lower panels in B). No MSP staining is seen in unmated females (right panels in B). The unmated control was overexposed to visualize the outline of the gonad. The relative fluorescence intensity of the MSP signal is shown in C. (D) The distance that the MSP signal extends from spermatozoa in mated females (*P<0.001, error bars represent s.d.). (E) The relative intensity of the MSP signal (fold above background) in the proximal gonad. *P<0.02, when compared to all the other measurements shown. $^{\dagger}P$>0.15, when compared with the other *emo-1(oz1)* mated female values, but P<0.05, when compared with the unmated female controls. (F) Punctate distribution of extracellular MSP. Projections of confocal 3D data stacks from mated females prepared by gonad dissection (left panel, MSP is red) or whole-mount fixation (right panel, MSP is pink and DNA is red). Large MSP puncta (arrows) are outside spermatozoa (s) in both the spermatheca (left panel, sp) and the uterus (u). More diffuse MSP fills the spermatheca (left panel) and extracellular spaces surrounding embryos (e, right panel). No MSP is observed in the distal gonad (dg). (G) MSP puncta (arrows) in close proximity to spermatozoa (s) in the uterus, detected by wide-field microscopy. Note the extended pseudopod (ps, bottom panels) and the sperm DNA (blue). Scale bars: B,C, 10 μm; F, 5 μm; G, 10 μm.

we observed MSP release from the labeled spermatozoa in all cases (Fig. 3C, *n*=12). By these criteria, the labeled spermatozoa were intact and functional, excluding lysis.

In addition, we generated antibodies to MSD-1 (F44D12.3), MSD-2 (F44D12.5), MSD-3 (F44D12.7) and MSD-4 (C35D10.11), identical members of a family of sperm-specific 11 kDa proteins containing an MSP domain distinct from that of MSP (referred to here collectively as MSD, for Major Sperm Domain proteins). The *Ascaris* ortholog, MFP1, is a component of the MSP cytoskeleton that decreases the rate of MSP fiber assembly in vitro (Buttery et al., 2003). We examined the localization of MSP and MSD in mated females by confocal microscopy and generated 3D-image reconstructions of the data. Although MSP and MSD exhibit extensive co-localization within the pseudopod and cell body of spermatozoa, only MSP localizes to extracellular puncta (Fig. 3D,E; Movies 5, 6 in the supplementary material). At the margins of the spermatozoa, we observed protrusions containing MSP but not MSD (Fig. 3E). These results suggest that MSP protrusions may give rise to free MSP puncta by a specific budding process, a possibility confirmed by electron microscopy (see below).

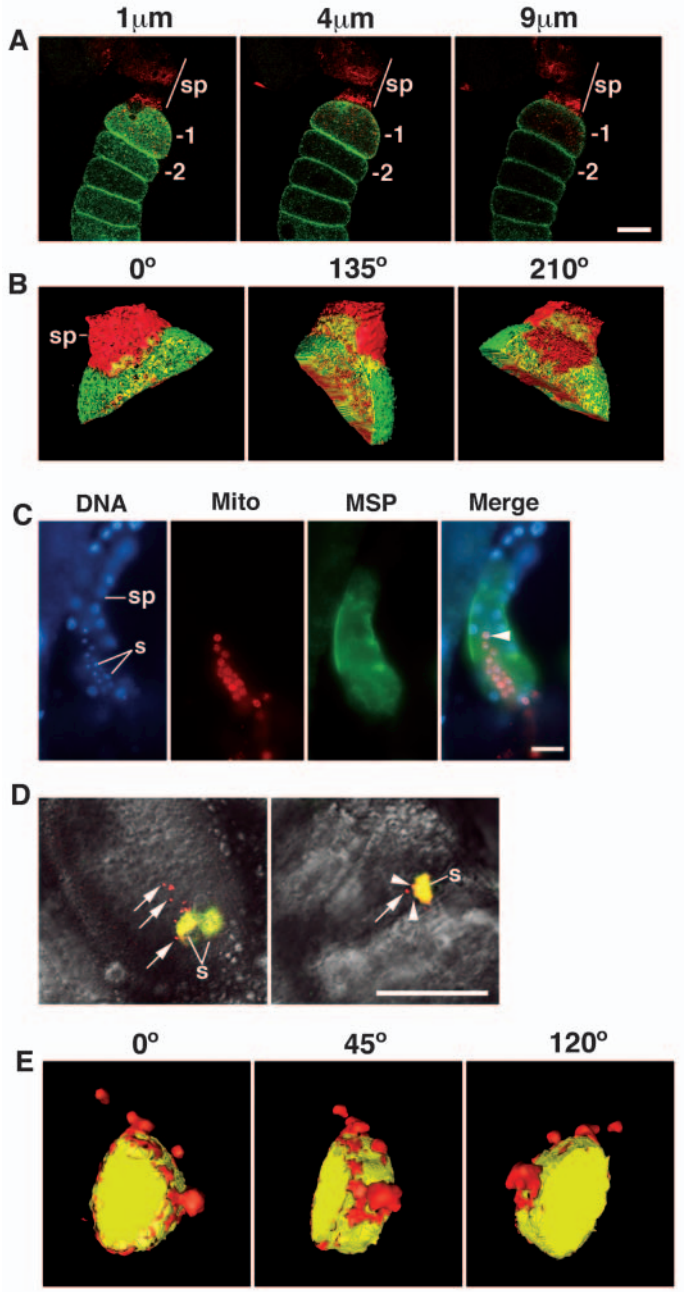

Release of MSP by vesicle budding

To address the mechanism of MSP release at an ultrastructural level, we used transmission electron microscopy (TEM) of adult hermaphrodites. In order to minimize processing artifacts and to get the best possible preservation of cell ultrastructure, we used high-pressure freezing and freeze substitution (HPF) techniques to prepare samples for TEM (McDonald, 1999; Müller-Reichert et al., 2003). The HPF method provided excellent morphology of germline and somatic tissues, including extracellular spaces in the spermatheca and uterus (Fig. 4). Using this approach, we detect novel 150-300 nm vesicles in extracellular spaces of the spermatheca (apical luminal regions) in close proximity to spermatozoa (Fig. 4A, left panel). These vesicles have not been observed in previous EM studies, which relied on conventional fixation techniques (L'Hernault, 1997) (data not shown). We analyzed vesicles in serial sections (*n*=30), and confirmed that they are free structures unattached to spermatozoa or somatic cells (Fig. 4B, and unpublished results). These vesicles have both an inner and an outer membrane. In serial sections, the central core narrows, and thus may be encapsulated by the inner membrane. By tilting the vesicles within the beam of the electron microscope,

Fig. 3. Localization of exported MSP and specificity of release. (A) Localization of MSP at the surface of the –1 oocyte. Single confocal sections at the indicated level of a 3D data stack through a mated female gonad stained for MSP (red) and RME-2 yolk receptor (green). No spermatozoa were seen in the indicated region (line) of the spermatheca (sp), thus the staining observed is extracellular to spermatozoa. A projection of the entire stack is presented as Movie 3 in the supplementary material. (B) Single angle views of a 3D reconstruction of the data stack represented in A. The image is cut to show surface and interior views of the –1 oocyte, at the indicated angles. Overlap between the MSP (red) and RME-2 (green) signals is yellow. Note the oocyte surface is slightly compressed where it abuts the spermatheca. The entire reconstruction is presented as Movie 4 in the supplementary material. (C) Intact and viable spermatozoa release MSP, as shown by a mated female stained for DNA (blue), MitoTracker (red) and MSP (green). Note, the MitoTracker staining is limited to the spermatozoa (s), but the MSP staining extends at least 50 μm from the most distal spermatozoa (arrowhead). (D) MSP localizes to extracellular puncta and apparent buds at the spermatozoa surface. Projections of confocal 3D data stacks from mated females stained in wholemount for MSP (red) and MSD proteins (green), with overlap in yellow. Images are superimposed on the DIC channel, showing spermatozoa (s) in the uterus. Puncta (arrows) and surface blebs (arrowheads) contain MSP, but not MSD proteins. A 3D projection of similar data is presented in Movie 5 in the supplementary material. (E) Budding generates MSP puncta. Single angle views of a 3D reconstruction of MSP (red) and MSD (green) staining, with overlap in yellow. The image is cut to show interior and surface views of the spermatozoa. Apparent sites of budding contain MSP but not MSD. The entire reconstruction is presented as Movie 6 in the supplementary material. Scale bars: 20 μm.

we were able to visualize inner and outer leaflets of both membranes (Fig. 4C). Tilting of the vesicles also indicates that they have a scalloped appearance formed by multiple bends of the outer membrane (Fig. 4D), and that the inner membrane is more regularly shaped (Fig. 4C). The annulus between the inner and outer membranes displays an electron density similar to the cytoplasm of spermatozoa. The inner core varies in appearance, containing irregular electron dense material (Fig. 4B-D). In addition to the spermatheca, we detect these vesicles in the uterine lumen, in extracellular spaces near spermatozoa (Fig. 4A, middle panel), and within extracellular crevices formed by close packing of embryos (Fig. 4A, right panel). Vesicles with this characteristic shape and morphology were not observed within the reproductive tract (gonad arm, spermatheca and uterus) of unmated females (Fig. 4E, and data not shown). Instead, the spermathecal and uterine lumens were filled with material similar to yolk lipoprotein particles, as described by Hall et al. (Hall et al., 1999) (Fig. 4E, and data not shown). These vesicles were not observed in extracellular (or cellular) spaces of other tissues (data not shown). Thus, EM analysis defines a novel class of extracellular vesicle associated with spermatozoa, which provides an attractive candidate at

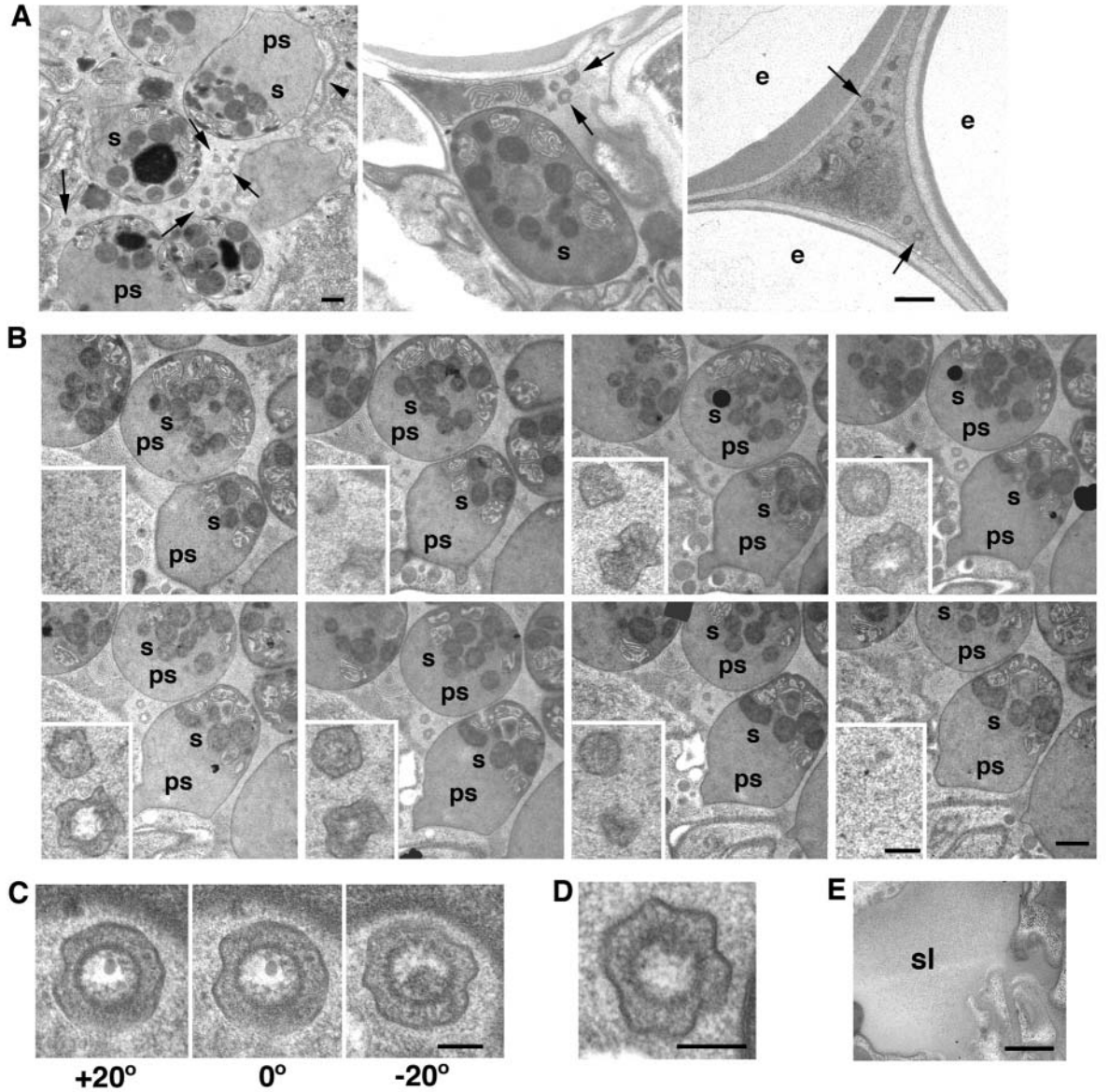

Fig. 4. Detection of a new class of vesicle by electron microscopy. (A) Low-power views of vesicles (arrows) in the extracellular space near spermatozoa (s) in the spermatheca (left), in the spermathecal-uterine junction region (middle), and in an extracellular space of the uterus formed by close packing of embryos (e; right). Pseudopods (ps) and an apical junction between spermathecal cells (arrowhead) are indicated. (B) Serial-section analysis of two vesicles in the spermatheca. Inset is a magnified view. Sections are 75 nm thick. (C) The vesicles possess two concentric lipid bilayers. Vesicles were tilted through the indicated angles in the EM beam to visualize the individual leaflets of the inner and outer membranes. (D) Tilting of a vesicle to visualize its scalloped appearance. (E) No MSP vesicles are observed in the spermathecal lumen (sl) of a *fog-2(q71)* female, instead the lumen is filled with material that resembles yolk lipoprotein particles. Scale bars: in A, 500 nm; in B, 125 nm; in C,D, 100 nm; in E, 500 nm.

the ultrastructural level for the MSP puncta described by fluorescence microscopy above.

To determine whether these novel vesicles contain MSP, we performed TEM on hermaphrodite samples prepared by HPF and post-embedding immunohistochemistry (immunoEM; Fig. 5). We observed strong labeling within the pseudopod and cell

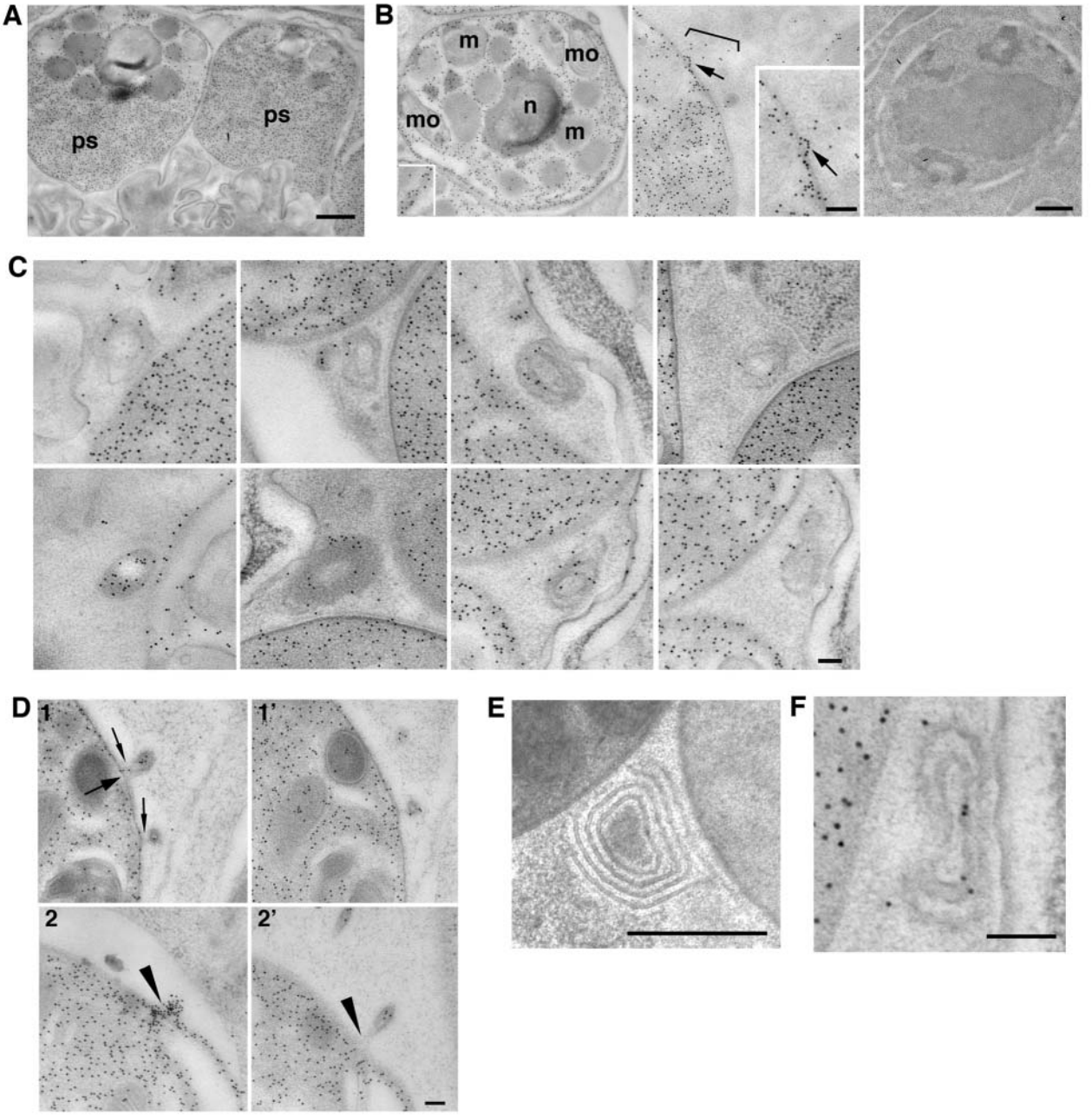

Fig. 5. Vesicles contain MSP and form by budding. (A) Detection of MSP by immunoEM. Low-power view of two spermatozoa in the spermathecal-uterine junction region of an adult hermaphrodite. Intense labeling in pseudopods (ps). (B) Detection of MSP at the plasma membrane of the spermatozoa cell body. (Left) MSP labeling excluded from cellular organelles, including mitochondria (m), membranous organelles (mo), and the nucleus (n). Inset is a magnified view showing MSP associated with the plasma membrane. (Middle) MSP associated with the plasma membrane and a protrusion (arrow), magnified in the inset. Note free labeling in the extracellular space (bracket). (Right) MSP is not detected in distal germ cells. (C) MSP is contained within the vesicles; a gallery of seven vesicles (the lower right two panels are views of the same vesicle in non-adjacent sections) is shown. MSP is located in the annulus between the inner and outer membranes. (D) Vesicle budding from spermatids. Shown are non-adjacent sections of two different spermatids in the hermaphrodite gonad. Views 1 and 1′, and 2 and 2′, are corresponding pairs of non-adjacent sections. The budding vesicles contain MSP in both views. Vesicles connect to the cell body by a stalk (thin arrows), and the plasma membrane at the budding site appears to be intact (thick arrow). MSP is enriched in a cross-sectional view at the base of the budding projection (arrowheads in lower panels). (E) Section of epon-embedded material showing a lipid whorl deposit in an extracellular space of the spermatheca between a portion of two spermatozoa. (F) MSP associated with a lipid whorl structure in the extracellular space of the spermatheca. Scale bar: in A, 500 nm; in B, 500 nm (inset, 125 nm); in C,D, 100 nm; in E, 500 nm; in F, 100 nm.

body of spermatozoa (Fig. 5A,B, left and middle panels). Within the cell body, MSP was enriched in close association with the plasma membrane (Fig. 5B, left panel and inset). We also detected small protrusions of the plasma membrane of the cell body containing MSP (Fig. 5B, middle panel and inset). By contrast, MSP labeling was largely excluded from the major cellular organelles of the spermatozoa, such as mitochondria, membranous organelles (MOs) and the nucleus (spermatozoa do not possess a nuclear envelope; Fig. 5A,B). No appreciable MSP labeling was observed in the distal germ line, the intestine, the body-wall muscle, spermathecal cells, uterine cells, or in *E. coli* surrounding the animal (Fig. 5B, right panel, and data not shown). Thus, detection of MSP by immunoEM was highly specific.

Using HPF followed by immunoEM, we detected MSP labeling of the novel vesicles in extracellular spaces of the spermatheca (Fig. 5C, 7 out of 9 vesicles labeled). Labeling was chiefly found within the annular ring between the inner and outer membranes. Because the only cells in the spermatheca and uterus observed to contain MSP are spermatozoa, these vesicles probably correspond to the MSP puncta, which apparently bud from them (see above). Consistent with this idea, we observed three cases of budding from spermatids in the gonad arm (Fig. 5D). Two buds were viewed in non-adjacent sections (Fig. 5D, top panels, views 1 and 1′). The buds exhibit MSP labeling in both views, and are connected to the cell body by a thin stalk (thin arrows) with the plasma membrane beneath the budding site apparently intact (thick arrow). A third example of vesicle budding from a spermatid in the gonad arm was found (Fig. 5D, bottom panels, views 2 and 2′), in which MSP intensely labeled the site of budding at the base of the projection in a circular pattern, possibly representing a cross-sectional view of a cylindrical network of MSP filaments (Fig. 5D, bottom left panel). Free MSP labeling in extracellular spaces could also be observed by immunoEM of adult hermaphrodites (Fig. 5B, middle panel), but it was generally less prevalent then when detected by immunofluoresence in mated females (see above). In adult hermaphrodites, we also observed unique lipid whorl deposits in the extracellular spaces of the spermatheca and uterus (Fig. 5E). These electron-dense whorls were not observed in the spermatheca or uterus of unmated females (Fig. 4E, and data not shown). In several cases, we observed MSP vesicles apparently fusing, possibly contributing the formation of the whorls (data not shown). Residual MSP labeling was associated with the lipid whorl deposits and thus they may represent an end fate of the MSP vesicles (Fig. 5F).

Spermatids and spermatozoa differ in temporal and spatial signaling properties

The development of both male and female gametes in the hermaphrodite gonad provides two contexts for MSP signaling. Spermatids signal nearby oocytes within the proximal gonad, whereas spermatozoa signal remotely from the spermatheca (Fig. 1). To compare the temporal and spatial signaling activities of spermatids and spermatozoa, we analyzed *spe-8(hc50)* and *spe-27(it110)* mutants, which are defective in hermaphrodite spermiogenesis. *spe-8* and *spe-27* mutants produce morphologically normal spermatids that can be activated for spermiogenesis and fertilization by male seminal fluid (L'Hernault, 1997). In the wild type, meiotic maturation rates progressively decline toward unmated female levels as spermatozoa run out (see Table S1 in the supplementary material). By contrast, *spe-8* and *spe-27* mutants exhibit maturation rates that are more constant over time (Table S1). This observation is surprising because the mutant spermatids are rapidly cleared from the reproductive tract (Fig. 6B, bottom) because they cannot crawl. To compare further the signaling potencies of spermatids and spermatozoa, we conducted a time-course analysis of MAPK activation (Fig. 6A). In the wild type, the percentage of gonad arms that exhibit MAPK activation in oocytes declines as sperm are used for fertilization, paralleling the decline in total MSP levels and sperm numbers (Fig. 6B). By contrast, in *spe-8* mutants, MAPK activation remains high at times (days 3 and 4) when sperm are depleted or no longer present. Consistent with this observation, residual MSP was faintly detected in *spe-8* mutants at these late times (Fig. 6B). As a control, we feminized *spe-8* (n=20) and *spe-27* (n=19) mutants using *fem-1(RNAi)*, which resulted in low meiotic maturation rates and a stacked oocyte phenotype comparable to *fog-2(q71)* females.

We next examined MSP release from spermatids. Wild-type, *spe-8*, and *spe-27* spermatids release MSP primarily in punctate form within the gonad arm (Fig. 6C,D; see also Movie 7 in the supplementary material; data not shown). MSP puncta appear to be widely distributed in wild-type and *spe-8* proximal gonad arms (Fig. 6C,D). By contrast, extracellular MSP produced by *spe-8* spermatids in the spermatheca appears more diffuse (Fig. 6C, top panels). At late times, we observed diffuse extracellular MSP in the spermatheca in *spe-8* mutants, despite the absence of spermatids (Fig. 6E). However, when spermatozoa are depleted in the wild type, no extracellular MSP is observed (see Fig. S1D,E in the supplementary material). This perdurance of extracellular MSP provides an explanation for the signaling observed at late times in *spe-8* and *spe-27* mutants. Taken together, these results suggest that spermatids provide a temporally long-acting form of the MSP-signal, whereas spermatozoa provide a long-range, temporally labile signal.

To investigate the potential basis for the increased stability of MSP signaling in *spe-8* mutants, we conducted HPF and TEM experiments. In *spe-8(hc50)* adult hermaphrodites, we observed MSP vesicles in the gonad arm, spermatheca and uterus (Fig. 7, and data not shown). The MSP vesicles were particularly abundant in the spermathecal-uterine junction region (Fig. 7A). In one respect, the MSP vesicles in *spe-8* mutants differed from those of the wild type (Fig. 4): the outer electron-dense layer of the *spe-8* MSP vesicles did not exhibit clearly distinguishable inner and outer leaflets (Fig. 7B,C, and data not shown). It is not clear whether this difference is a consequence of their increased stability, or whether it represents some fundamental difference in their assembly. One observation in *spe-8* mutants, however, may shed some additional light on how the MSP vesicles may form. In fertilization-defective mutants, such as *spe-8(hc50)*, the unfertilized oocytes sometimes lyse in the spermatheca or uterus because they do not form egg shells. In these cases, oocyte cytoplasm and organelles filled the spermathecal lumen (Fig. 7C), and we observed that the interior of the MSP vesicles contained material markedly similar to that found in the extracellular space (Fig. 7C). This observation suggests that the

internal ring of the MSP vesicle may derive from the extracellular space, a possibility that will require further experiments to address it fully.

Because *spe-8* mutants do not form pseudopods, we examined the morphology of the cell body in detail to uncover additional information related to the formation of the MSP vesicles. As seen for wild-type spermatids (Fig. 5D), we observed protrusions of the plasma membrane (Fig. 7D-I). These varied in length from 100 nm to 2 μm in size (Fig. 7D-I, and data not shown), and often had a bent appearance (Fig. 7E). These protrusions contained MSP labeling (Fig. 7F,I). Often, pairs of closely spaced protrusions formed in close proximity to one another (Fig. 7G-I). These observations provide additional evidence for a vesicle-budding process at the cell body of spermatids and spermatozoa, and raise the issue of whether closely spaced buds may contribute to the formation of MSP vesicles.

The data presented above provide evidence that spermatids and spermatozoa release MSP via a vesicle-budding process. Although sperm lack an ER and a Golgi, they may have relocated their protein translocation apparatus to the plasma membrane, as in prokaryotes. To test this possibility, we examined MSP localization in *emo-1/sec-61γ(oz1)* hermaphrodites (n=23), which are defective for secretion in the germ line (Iwasaki et al., 1996). We observed that *emo-1(oz1)* spermatids generate extracellular MSP in both punctate and diffuse forms (see Fig. S2 in the supplementary material). This observation provides further support for the idea that MSP release is independent of the traditional secretory pathway.

Because spermatids release MSP, motility and a pseudopod

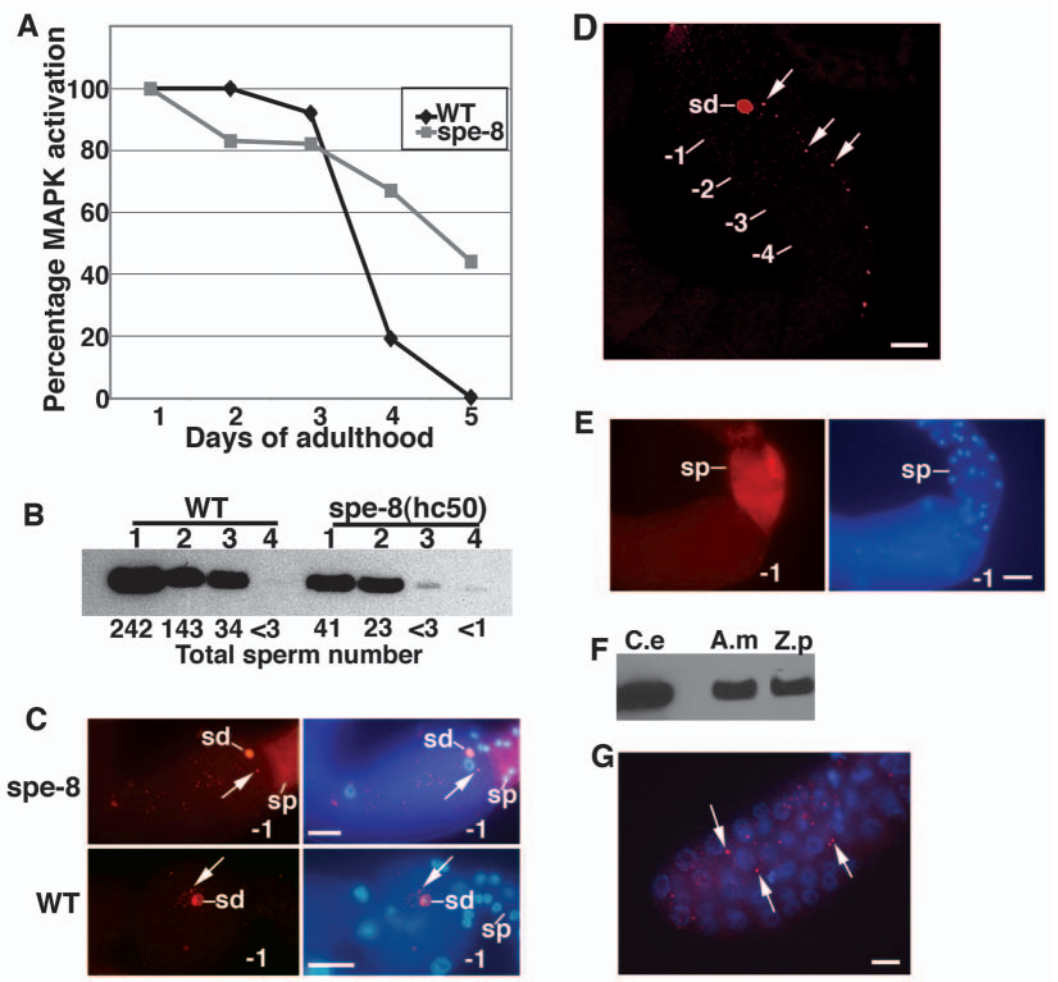

Fig. 6. Spermatids provide a long-acting MSP signal. (A) Time-course analysis of MAPK activation in the wild type and *spe-8(hc50)* mutants. The percentage of gonad arms with activated MAPK was measured by staining dissected gonads at the indicated times of adulthood. (B) Time course of total MSP levels analysed by western blots of MSP in *spe-8(hc50)* and the wild type (10 animals/lane). The number of spermatids and spermatozoa were counted at each time point. The data represents the average of three trials. (C) Detection of MSP puncta (arrows) located near spermatids (sd) in the proximal gonad arm of *spe-8(hc50)* and wild-type hermaphrodites. MSP (red) and DNA (blue) were detected. MSP is detected in the spermatheca (sp) of *spe-8(hc50)* hermaphrodites, but no spermatids are observed. (D) Projection of a confocal 3D-data stack showing MSP puncta (arrow) distributed widely in the proximal gonad, far from the single *spe-8(hc50)* spermatid (sd) that can be seen. (E) MSP perdures in *spe-8(hc50)* mutants. MSP (red) staining is observed, but spermatids are not, confirmed by viewing the DNA (blue) signal in multiple focal planes. (F) Western blot of MSP in *C. elegans* (C.e), and the Cephalobid nematodes *Acrobeloides maximus* (A.m) and *Zeldia punctata* (Z.p). (G) Detection of MSP puncta (arrows) in the *A. maximus* gonad. Only the distal arm is shown. Scale bars: in C, 20 μm; in D, 10 μm; in E,G, 20 μm.

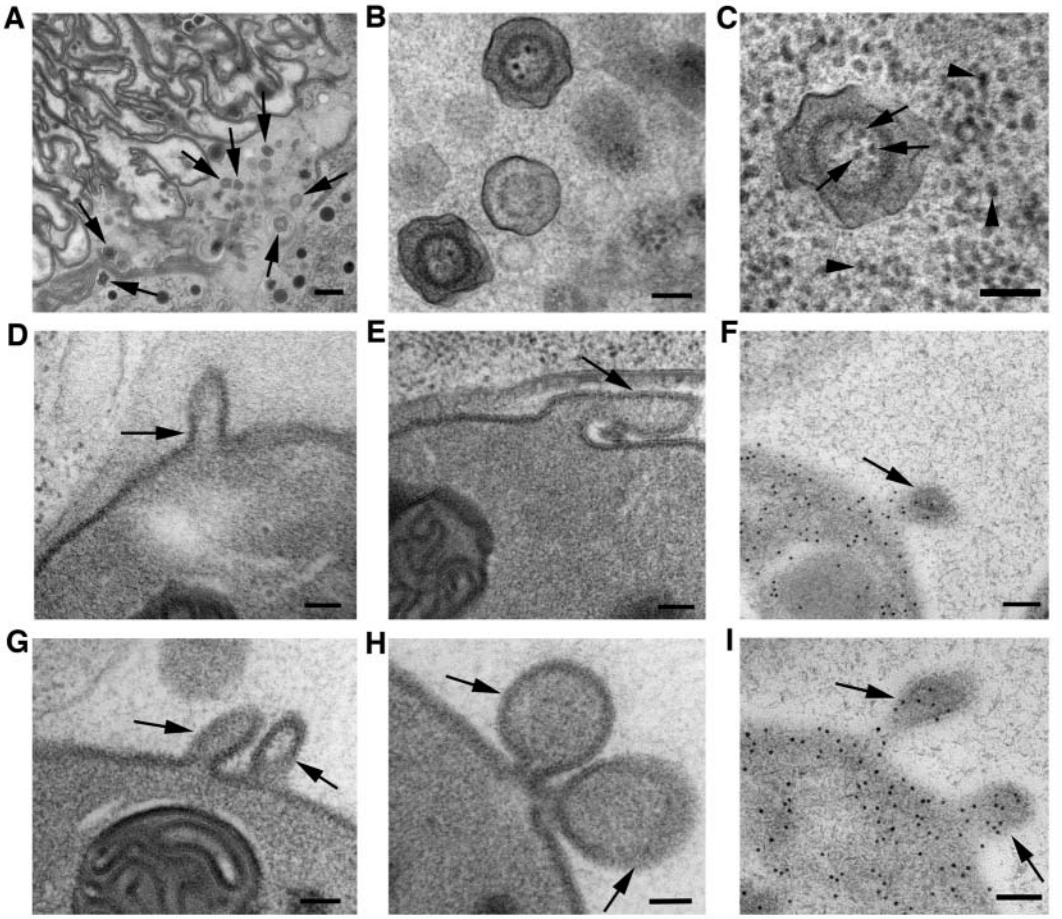

Fig. 7. Production of MSP vesicles in the spermiogenesis-defective *spe-8(hc50)* mutant. (A) Low-power view of the spermathecal-uterine junction region. MSP vesicles (arrows) are abundant in extracellular spaces of this region. (B) High-magnfication view of MSP vesicles located in the region shown in A, from an adjacent section. (C) MSP vesicle in the spermathecal lumen surrounded by cytoplasmic debris from a lysed oocyte (arrowheads). Note, the inner ring of the MSP vesicle contains material (arrows) similar to the oocyte cytoplasmic contents. (D-I) Protrusions (arrows) from the cell body of spermatids located in the gonad arm. (F,I) Detection of MSP in protrusions. Scale bars: in A, 500 nm; in B-I, 100 nm.

are dispensable. This result prompted us to examine whether parthenogenetic nematodes, which reproduce without sperm, have MSP. We analyzed the highly divergent Cephalobid parthenogens *Acrobeloides maximus* and *Zeldia punctata* using monoclonal antibodies raised to the highly conserved MSP C terminus. We detected MSP by western blot of both *A. maximus* and *Z. punctata* (Fig. 6F). Immunostaining of *A. maximus* indicated that punctate immunoreactivity was widely distributed in the female germline (Fig. 6G, and data not shown). Although the functional roles of MSP in *A. maximus* and *Z. punctata* will require additional study, these results indicate that MSP can be conserved in evolution for functions unrelated to the motility of spermatozoa.

Discussion

A vesicle-budding mechanism for MSP release

Here we provide evidence that *C. elegans* sperm use a novel vesicle-budding mechanism to deliver the MSP signal to oocytes and sheath cells. We used an array of microscopic modalities and multiple specific antibodies to examine MSP localization in mated females and hermaphrodites. In particular, mated females provide an ideal format for analyzing MSP release because spermatozoa, and thus MSP, are supplied entirely by mating. As the distal constriction of the spermatheca constitutes a barrier to sperm entry, staining in the proximal gonad is due to MSP that is extracellular to spermatozoa. Using fluorescence microscopy, we observed two forms of extracellular MSP: a punctate form and a diffuse form. Three observations suggest that MSP puncta may represent the precursor to the diffuse form. First, confocal microscopy provides evidence for budding of MSP puncta from spermatozoa, thereby identifying their origin. Second, the punctate form is absent from the proximal gonad arm of mated females, whereas the diffuse form can reach the responding oocytes. Third, when spermatids have been cleared from the reproductive tract in spermiogenesis defective mutants, only the diffuse form is observed.

Several lines of evidence rule out alternative explanations for these observations, such as lysis, or leaching of proteins from spermatids and spermatozoa during fixation. First, MSP release is highly specific, as abundant and soluble sperm-specific components of the MSP cytoskeleton, the MSD proteins, are not observed in MSP puncta or in buds. Second, vital dye-labeling experiments indicate that spermatozoa remain intact and functional, despite releasing MSP. Third, in spermiogenesis-defective hermaphrodites, after spermatids clear from the reproductive tract, extracellular MSP staining is still detected, and thus must originate prior to fixation. Fourth, multiple MSP antibodies and fixation conditions yield consistent results. Finally, electron and light microscopy paint congruent pictures of MSP release.

Using TEM, we detected a new class of vesicle, the MSP vesicle, in the spermatheca and uterus of adult hermaphrodites. ImmunoEM demonstrates that these vesicles contain MSP and probably correspond to the MSP puncta observed by confocal

microscopy. The observation that MSP vesicles are more abundant in *spe-8* mutants, which produce a long-acting MSP signal, provides correlative data that MSP vesicles may represent signaling intermediates. While the precise steps and dynamics by which the MSP vesicles form remain to be determined, our static observations are consistent with the possibility that protrusions from the cell body may bend back upon themselves and pinch off, thereby encapsulating lumenal material within a double-membraned vesicle (see Fig. S3 in the supplementary material). MSP vesicles are likely to be labile structures because they are not detectable by conventional electron microscopy and they appear to fuse to generate lipid whorls. Thus, instability of the MSP vesicles may liberate MSP in a free form able to bind oocytes and sheath cells via the VAB-1 Eph receptor protein-tyrosine kinase and other unidentified receptors (Miller et al., 2003). Taken together then, these results suggest that MSP release from spermatozoa and spermatids occurs in two stages: (1) budding of MSP vesicles; and (2) vesicle disintegration. As both spermatids and spermatozoa release MSP via vesicle budding, neither a pseudopod nor motility is required.

Vesicle budding, a nexus for the motility and signaling functions of MSP

Does vesicle budding use activities of MSP that are also required for amoeboid locomotion of nematode spermatazoa? Several features of MSP vesicle budding suggest this is indeed the case. ImmunoEM shows that MSP is enriched at, and associated with, the plasma membrane of the cell body of spermatids and spermatozoa. Localized MSP filament assembly may generate the protrusive force driving vesicle budding at the plasma membrane of the cell body, analogous to the leading edge protrusion that drives pseudopodial extension (Italiano et al., 1996; Bottino et al., 2002). Consistent with this idea, we observed MSP in protrusions of the plasma membrane of the cell body by immunoEM (Figs 5, 7). Confocal microscopy and 3D-image reconstructions identify MSP-containing protrusions, which are likely to correspond to the sites of budding. Whereas MSP is concentrated at these budding sites, the MSD proteins are absent. In vitro studies of MSP-based motility in *Ascaris* identified MFD1, the ortholog of the MSD proteins, as having an activity that decreases the rate of MSP fiber growth (Buttery et al., 2003). Thus, the absence of the MSD proteins at the vesicle-budding sites may favor MSP filament assembly and membrane protrusion.

In vesicle-budding processes, bending of the lipid bilayer is energetically costly because of a strong hydrophobic effect (Chernomordik and Kozlov, 2003). It is likely that the TEM views of the vesicle-budding process demonstrate the involvement of bent and looped intermediates (Figs 5, 7). Several observations provide initial indications of how membrane bending may be achieved during vesicle budding. Localized polymerization of MSP filaments may provide the protrusive force that drives membrane bending. MSP filaments are flexible and have a short persistence length, and are thus conducive to bending (Italiano et al., 1996; Bottino et al., 2002). TEM views of MSP vesicles indicate that they have a regular, highly bent, scalloped appearance, suggesting the involvement of vesicle-coating proteins. Thus, MSP polymerization may provide the energy driving membrane protrusion and bending, while uncharacterized coat proteins may store this energy and stabilize the bent configuration. As MSP cytoskeletal dynamics powers retraction in amoeboid motility (Miao et al., 2003), an attractive idea is that disassembly of MSP filaments at the base of the projection may play a role in scission.

How is MSP vesicle budding regulated? Vesicle budding results in loss of MSP and plasma membrane from spermatids and spermatozoa; therefore, there must be a trade-off between MSP signaling and motility. The best evidence that MSP vesicle budding is regulated comes from two sets of related observations: first, MSP release does not occur from spermatids within or dissected from males; and second, extracts of female animals promote vesicle budding from spermatids in vitro (data not shown). The possibility that MSP release may depend on extracellular cues from the hermaphrodite reproductive tract may have precedents in MSP-based motility, because spermatozoa are likely to sense directional cues as they navigate from the uterus to the spermatheca. In this view then, MSP cytoskeletal dynamics would drive pseudopodial extension and crawling in response to one set of cues, and vesicle budding in response to another. Alternatively, a single signal from the hermaphrodite could elicit vesicle budding and directional movement by activating divergent downstream effectors. Identification of the putative cues will provide the most direct test of these hypotheses.

Vesicle budding provides a basis for long- and short-range MSP signaling

Our results suggest two modes of MSP signaling: spermatids appear to provide a temporally long-acting form of the MSP signal; and spermatozoa provide a long-range, labile signal. This plasticity is well adapted for the developmental stages of MSP signaling. Spermatids signal neighboring oocytes from within the gonad, and spermatozoa must signal from far-flung regions including the spermatheca and the uterus. For the sperm-sensing mechanism (Miller et al., 2003) to generate a biologically meaningful output, extracellular MSP levels must be valid and reliable indicators of sperm availability. A block to spermiogenesis short-circuits the control mechanism.

Our results suggest that differential MSP vesicle stability may provide a mechanistic basis for the distinct signaling activities of spermatids and spermatozoa. In *spe-8* mutants, MSP vesicles are more stable, and signaling persists after the spermatids are swept from the reproductive tract by ovulated oocytes. While it is not possible to completely exclude the possibility that *spe-8* mutant spermatids release the MSP signal in a qualitatively or quantitatively different manner from wild-type spermatids in the gonad, the isolation of a large class of sperm-defective mutants on the basis that they lay unfertilized oocytes in high quantity suggests that many mutants that disrupt spermiogenesis may have this property (L'Hernault, 1997). If wild-type spermatids do indeed produce a long-acting signal within the gonad arm, then some mechanism must exist to eliminate this form of the MSP signal after ovulations have commenced and the spermatids have entered the spermatheca and undergone spermiogenesis. Otherwise, meiotic maturation might continue at a brisk pace after sperm are depleted and thus oocytes would be wasted. Possibly, the presence of spermatozoa may destabilize MSP vesicles from spermatids in trans. Although the actual determinants of MSP vesicle stability are unclear, both intrinsic and extrinsic factors

may contribute. During spermiogenesis, ER/Golgi-derived organelles, the membranous organelles (MOs), fuse with the plasma membrane to transfer their contents to the cell surface and the extracellular environment (L'Hernault, 1997; Xu and Sternberg, 2003). MO fusion is not required for the budding process because spermatids, which have unfused MOs bud vesicles, and *fer-1* mutants, which are defective in MO fusion (Achanzar and Ward, 1997), are able to signal (McCarter et al., 1999). Nonetheless, MO fusion generates a difference between the plasma membrane protein composition of spermatids and spermatozoa that might affect the stability of their respective MSP vesicles.

MSP vesicle budding and unconventional secretory mechanisms

How general is the MSP vesicle-budding mechanism? MSPs are highly conserved in nematodes where they play both cytoskeletal and signaling roles. Proteins with MSP domains are also found in fungi, plants and animals. Genetic studies demonstrate that a MSP domain protein, DVAP-33A, functions as an instructive signal during bouton formation at the neuromuscular junction in *Drosophila* (Pennetta et al., 2002). A mutation in the MSP domain of VAPB causes late-onset spinal muscular atrophy and amyotrophic lateral sclerosis type 8 in humans (Nishimura et al., 2004). Our observation that MSP localizes to membranes and apparently drives vesicle budding may define a general activity for the MSP domain in other proteins.

As a molecular mechanism, vesicle budding provides a general means for releasing cytoplasmic proteins from cells. It is now becoming clear that diverse intracellular proteins can be secreted from cells by novel means, independent of a signal peptide or the ER/Golgi system (Nickel, 2003). Proteins released by non-classical secretory pathways fit into two broad groups: those that are located within vesicular compartments within the cell; and those that are cytoplasmic. For example, IL-1β is associated with secretory lysozymes and is released by an unconventional mechanism (Stinchcombe et al., 2004). By contrast, galectin 1 and 3 (Cooper and Barondes, 1990), fibroblast growth factors 1 and 2 (Mignatti et al., 1992), and HIV-Tat (Chang et al., 1997) are probably cytoplasmic, yet are exported from cells. For some members of both groups (e.g. IL-1β, galectin 1, FGF-2), there is evidence for release within vesicles (Cooper and Barondes, 1990; MacKenzie et al., 2001).

With classical ER/Golgi-dependent protein secretion mechanisms so robust, it is reasonable to ask why cells should bother with unconventional export pathways? In the case of MSP, nematode spermatids and spermatozoa simply do not have any other option, having jettisoned their ribosomes, ER/Golgi and actin during meiosis II. A similar argument explains why spermatozoa from many vertebrate and invertebrate species rely on the acrosome reaction for zona penetration. A variety of highly specialized cells (e.g. melanocytes, platelets, cytotoxic T-lymphocytes, mammary gland cells and sweat gland cells) rely on unconventional protein export pathways (Nickel, 2003; Stinchcombe et al., 2004). Possibly, non-canonical secretion mechanisms provide highly specialized cells with a greater flexibility in dynamic environments in which the cell positions or developmental status are changeable, as for MSP vesicle budding.

This paper is dedicated to the memory of Peter A. Kolodziej, our colleague and friend, whose scientific contributions will not be forgotten. Thanks to *Caenorhabditis* Genetics Center, Paul De Ley, David Fitch, Barth Grant, Jane Hubbard, Steve L'Hernault, Tom Roberts, Tim Schedl, Andrew Singson and Sam Ward for strains and reagents; Jay Jerome, Gary Olson and Ginger Winfrey for help with electron microscopy; David King for guidance on antibody methods and peptide design; Heping Yan and Ray Mernaugh for help with monoclonal antibodies; and Michael Anderson and Jonathan Holder for technical assistance. Thanks to Denise Lapidus for growing and maintaining worms prior to freezing. Special thanks to Kathy Gould, David Hall, Peter Kolodziej, Steve L'Hernault, David Miller, Millet Treinin and Michael Miller for helpful suggestions, comments on the manuscript, and encouragement. This work was supported by NIH grants GM57173 and GM65115 (D.G.), NIH Training Grant T32 CA09592 (M.K.), and by NIH grants 5P30 CA68485 and 5P30 ES00267, which support the Molecular Recognition Shared Resource.

Supplementary material

Supplementary material for this article is available at
http://dev.biologists.org/cgi/content/full/132/15/3357/DC1

References

Achanzar, W. E. and Ward, S. (1997). A nematode gene required for sperm vesicle fusion. *J. Cell Sci.* **110**, 1073-1081.

Bottino, D., Mogilner, A., Roberts, T., Stewart, M. and Oster, G. (2002). How nematode sperm crawl. *J. Cell Sci.* **115**, 367-384.

Buttery, S. M., Ekman, G. C., Seavy, M., Stewart, M. and Roberts, T. M. (2003). Dissection of the *Ascaris* sperm motility machinery identifies key proteins involved in major sperm protein-based amoeboid locomotion. *Mol. Biol. Cell* **14**, 5082-5088.

Chang, H. C., Samaniego, F., Nair, B. C., Buonaguro, L. and Ensoli, B. (1997). HIV-1 Tat protein exits from cells via a leaderless secretory pathway and binds to extracellular matrix-associated heparan sulfate proteoglycans through its basic region. *AIDS* **11**, 1421-1431.

Chernomordik, L. V. and Kozlov, M. M. (2003). Protein-lipid interplay in fusion and fission of biological membranes. *Annu. Rev. Biochem.* **72**, 175-207.

Cooper, D. N. and Barondes, S. H. (1990). Evidence for export of a muscle lectin from cytosol to extracellular matrix and for a novel secretory mechanism. *J. Cell Biol.* **110**, 1681-1691.

De Ley, P., Geraert, E. and Coomans, A. (1990). Seven cephalobids from Senegal. *J. Afr. Zool.* **104**, 287-304.

Eisenbach, M. and Tur-Kaspa, I. (1999). Do human eggs attract spermatozoa? *BioEssays* **21**, 203-210.

Grant, B. and Hirsh, D. (1999). Receptor-mediated endocytosis in the *Caenorhabditis elegans* oocyte. *Mol. Biol. Cell* **10**, 4311-4326.

Hall, D. H., Winfrey, V. P., Blaeuer, G., Hoffman, L. H., Furuta, T., Rose, K. L., Hobert, O. and Greenstein, D. (1999). Ultrastructural features of the adult hermaphrodite gonad of *Caenorhabditis elegans*: relations between the germ line and soma. *Dev. Biol.* **212**, 101-123.

Hardy, D. M. (ed.) (2002). *Fertilization*. San Diego: Academic Press.

Harlow, E. and Lane, D. (1988). *Antibodies: A Laboratory Manual*. New York: Cold Spring Harbor Laboratory Press.

Hill, K. L. and L'Hernault, S. W. (2001). Analyses of reproductive interactions that occur after heterospecific matings within the genus *Caenorhabditis*. *Dev. Biol.* **232**, 105-114.

Howe, M., McDonald, K. L., Albertson, D. G. and Meyer, B. J. (2001). HIM-10 is required for kinetochore structure and function on *Caenorhabditis elegans* holocentric chromosomes. *J. Cell Biol.* **153**, 1227-1238.

Hubbard, E. J. and Greenstein, D. (2000). The *Caenorhabditis elegans* gonad: a test tube for cell and developmental biology. *Dev. Dyn.* **218**, 2-22.

Italiano, J. E., Jr, Roberts, T. M., Stewart, M. and Fontana, C. A. (1996). Reconstitution in vitro of the motile apparatus from the amoeboid sperm of *Ascaris* shows that filament assembly and bundling move membranes. *Cell* **84**, 105-114.

Iwasaki, K., McCarter, J., Francis, R. and Schedl, T. (1996). *emo-1*, a *Caenorhabditis elegans* Sec61p gamma homologue, is required for oocyte development and ovulation. *J. Cell Biol.* **134**, 699-714.

Kamath, R. S., Martinez-Campos, M., Zipperlen, P., Fraser, A. G. and

Ahringer, J. (2001). Effectiveness of specific RNA-mediated interference through ingested double-stranded RNA in *Caenorhabditis elegans*. *Genome Biol.* **2**, 1-10.
Klass, M. R. and Hirsh, D. (1981). Sperm isolation and biochemical analysis of the major sperm protein from *C. elegans*. *Dev. Biol.* **84**, 299-312.
L'Hernault, S. (1997). Spermatogenesis. In C. elegans *II* (ed. D. L. Riddle, T. Blumenthal, B. J. Meyer and J. R. Priess), pp. 271-294. New York: Cold Spring Harbor Laboratory Press.
L'Hernault, S. W., Shakes, D. C. and Ward, S. (1988). Developmental genetics of chromosome I spermatogenesis-defective mutants in the nematode *Caenorhabditis elegans*. *Genetics* **120**, 435-452.
Lonsdale, J. E., McDonald, K. L. and Jones, R. L. (1999). High pressure freezing and freeze substitution reveal new aspects of fine structure and maintain protein antigenicity in barley aleurone cells. *Plant J.* **17**, 221-229.
Lonsdale, J. E., McDonald, K. L. and Jones, R. L. (2001). Microwave polymerization in thin layers of LR white allows selection of specimens for immunogold labeling. In *Microwave Techniques and Protocols* (ed. R. T. Giberson and R. S. Demaree, Jr), pp. 139-153. New Jersey: Humana Press.
MacKenzie, A., Wilson, H. L., Kiss-Toth, E., Dower, S. K., North, R. A. and Surprenant, A. (2001). Rapid secretion of interleukin-1beta by microvesicle shedding. *Immunity* **15**, 825-835.
Masui, Y. (1985). Meiotic arrest in animal oocytes. In *Biology of Fertilization* (ed. C. B. Metz and A. Monroy), pp. 189-219. Florida: Academic Press.
McCarter, J., Bartlett, B., Dang, T. and Schedl, T. (1999). On the control of oocyte meiotic maturation and ovulation in *Caenorhabditis elegans*. *Dev. Biol.* **205**, 111-128.
McDonald, K. (1999). High-pressure freezing for preservation of high resolution fine structure and antigenicity for immunolabeling. *Methods Mol. Biol.* **117**, 77-97.
Miao, L., Vanderlinde, O., Stewart, M. and Roberts, T. M. (2003). Retraction in amoeboid cell motility powered by cytoskeletal dynamics. *Science* **302**, 1405-1407.
Miller, M. A., Nguyen, V. Q., Lee, M. H., Kosinski, M., Schedl, T., Caprioli, R. M. and Greenstein, D. (2001). A sperm cytoskeletal protein that signals oocyte meiotic maturation and ovulation. *Science* **291**, 2144-2147.
Miller, M. A., Ruest, P. J., Kosinski, M., Hanks, S. K. and Greenstein, D. (2003). An Eph receptor sperm-sensing control mechanism for oocyte meiotic maturation in *Caenorhabditis elegans*. *Genes Dev*. **17**, 187-200.
Mignatti, P., Morimoto, T. and Rifkin, D. B. (1992). Basic fibroblast growth factor, a protein devoid of secretory signal sequence, is released by cells *via* a pathway independent of the endoplasmic reticulum-Golgi complex. *J. Cell Physiol*. **151**, 81-93.
Müller-Reichert, T., O'Toole, E. T., Hohenberg, H. and McDonald, K. L. (2003). Cryoimmobilization and three-dimensional visualization of *C. elegans* ultrastructure. *J. Microsc*. **212**, 71-80.
Neill, A. T. and Vacquier, V. D. (2004). Ligands and receptors mediating signal transduction in sea urchin spermatozoa. *Reproduction* **127**, 141-149.
Nickel, W. (2003). The mystery of nonclassical protein secretion. A current view on cargo proteins and potential export routes. *Eur. J. Biochem*. **270**, 2109-2119.
Nishimura, A. L., Mitne-Neto, M., Silva, H. C. A., Richieri-Costa, A., Middleton, S., Cascio, D., Kok, F., Oliveira, J. R. M., Gillingwater, T., Webb, J., Skehel, P. and Zatz, M. (2004). A mutation in the vesicle-trafficking protein VAPB causes late-onset spinal muscular atrophy and amyotrophic lateral sclerosis. *Am. J. Genet.* **75**, 822-831.
Nonet, M. L., Staunton, J. E., Kilgard, M. P., Fergestad, T., Hartwieg, E., Horvitz, H. R., Jorgensen, E. M. and Meyer, B. J. (1997). *Caenorhabditis elegans rab-3* mutant synapses exhibit impaired function and are partially depleted of vesicles. *J. Neurosci*. **17**, 8061-8073.
Pennetta, G., Hiesinger, P., Fabian-Fine, R., Meinertzhagen, I. and Bellen, H. J. (2002). *Drosophila* VAP-33A directs bouton formation at neuromuscular junctions in a dosage-dependent manner. *Neuron* **32**, 291-306.
Riddle, D. L., Blumenthal, T., Meyer, B. J. and Priess, J. R. (eds) (1997). *C. elegans II*. New York: Cold Spring Harbor Laboratory Press.
Rose, K. L., Winfrey, V. P., Hoffman, L. H., Hall, D. H., Furuta, T. and Greenstein, D. (1997). The POU gene *ceh-18* promotes gonadal sheath cell differentiation and function required for meiotic maturation and ovulation in *Caenorhabditis elegans*. *Dev. Biol.* **192**, 59-77.
Spehr, M., Gisselmann, G., Poplawski, A., Riffell, J. A., Wetzel, C. H., Zimmer, R. K. and Hatt, H. (2003). Identification of a testicular odorant receptor mediating human sperm chemotaxis. *Science* **299**, 2054-2058.
Stinchcombe, J., Bossi, G. and Griffiths, G. M. (2004). Linking albinism and immunity: the secrets of secretory lysosomes. *Science* **305**, 55-59.
Thorne, G. (1925). The genus *Acrobeles* von Linstow, 1877. *Trans Am. Microsc. Soc.* **44**, 171-209.
Ward, G. E., Brokaw, C. J., Garbers, D. L. and Vacquier, V. D. (1985). Chemotaxis of *Arbacia punctulata* spermatozoa to resact, a peptide from the egg jelly layer. *J. Cell Biol*. **101**, 2324-2329.
Ward, S. and Carrel, J. S. (1979). Fertilization and sperm competition in the nematode *Caenorhabditis elegans*. *Dev. Biol.* **73**, 304-321.
Ward, S. and Klass, M. (1982). The location of the major protein in *C. elegans* sperm and spermatocytes. *Dev. Biol*. **92**, 203-208.
Ward, S., Roberts, T. M., Strome, S., Pavalko, F. M. and Hogan, E. (1986). Monoclonal antibodies that recognize a polypeptide antigenic determinant shared by multiple *C. elegans* sperm-specific proteins. *J. Cell Biol.* **102**, 1778-1786.
Wassarman, P. M., Jovine, L. and Litscher, E. S. (2001). A profile of fertilization in mammals. *Nat. Cell Biol.* **3**, E59-E64.
Xu, X. Z. and Sternberg, P. W. (2003). A *C. elegans* sperm TRP protein required for sperm-egg interactions during fertilization. *Cell* **114**, 285-297.

Table S1. Time-course analysis of MSP signaling

Genotype*	Meiotic maturation rates (maturations per gonad arm per hour)				
	1-day adult	2-day adult	3-day adult	4-day adult	5-day adult
fog-2(q71)	0.07±0.07 (*n*=18)	0.17±0.13 (*n*=18)	0.22±0.20 (*n*=18)	0.20±0.20 (*n*=18)	0.21±0.16 (*n*=19)
Wild type	2.23±0.67† (*n*=30)	2.87±0.57† (*n*=30)	1.38±0.83† (*n*=30)	0.82±0.54† (*n*=28)	0.30±0.30‡ (*n*=26)
Wild type mated on day 3	N. A.	N. A.	N. A.	2.32±0.82†,§ (*n*=37)	1.68±0.73†,§ (*n*=42)
fog-2(q71) mated	1.80±0.41†,¶ (*n*=32)	2.63±0.58†,** (*n*=30)	2.71±0.73†,§ (*n*=30)	2.47±0.95†,§ (*n*=29)	1.51±0.87†,§ (*n*=26)
tra-3(e2333)	1.77±0.38†,¶ (*n*=34)	2.40±0.54†,¶ (*n*=25)	2.30±0.63†,§ (*n*=28)	1.22±0.40†,§ (*n*=24)	0.56±0.43§,†† (*n*=19)
spe-9(eb19)	1.17±0.73†,§ (*n*=18)	1.98±0.69†,** (*n*=18)	2.17±0.50†,§ (*n*=14)	2.35±0.53†,§ (*n*=12)	1.73±0.64†,§ (*n*=16)
spe-8(hc50)	1.73±0.67†,‡‡ (*n*=20)	1.35±0.82†,§ (*n*=20)	0.99±0.60†,** (*n*=30)	0.64±0.55**,†† (*n*=28)	0.94±0.66†,§ (*n*=21)
spe-8(hc50) mated	N. D.	N. D.	N. D.	N. D.	2.27±0.90†,§ (*n*=10)
spe-27(it110)	1.54±0.84†,¶ (*n*=20)	1.01±0.43†,‡‡ (*n*=20)	1.27±0.68†,§§ (*n*=30)	1.05±0.58†,** (*n*=30)	0.90±0.62†,§ (*n*=32)

Maturation rates were measured in 5-hour intervals at various times after mid-L4 stage. Standard deviations are shown. Statistical significance was assessed using Student's *t*-test.

N. A., not applicable; N. D., not done.

*Genotypes analyzed: *fog-2(q71)* produce no sperm; *tra-3(e2333)* produce approximately 50% more sperm (Hodgkin and Barnes, 1991); *spe-9(eb19)* are defective in fertilization; *spe-8(hc50)* and *spe-27(it110)* produce non-motile spermatids lacking a pseudopod (Singson et al., 1998).

$^{\dagger}P<0.001$, $^{\dagger\dagger}P<0.01$, and $^{\ddagger}P>0.5$, compared with *fog-2(q71)* female values at the same time point.

$^{\S}P<0.001$, $^{\P}P<0.01$, $^{\ddagger\ddagger}P<0.05$, $^{**}P>0.2$, and $^{\S\S}P>0.5$, compared with wild-type hermaphrodite values at the same time point.

Summary of meiotic maturation time-course measurements. (1) Meiotic maturation rates are fine-tuned to the number of spermatozoa present (compare *fog-2(q71)*, wild type and *tra-3(e2333)*). (2) Spermatozoa must signal continuously because rates remain high in the fertilization-defective *spe-9* mutant (*spe-9(eb19)*). (3) Spermatids produce a long-acting signal, which persists after the *spe-8* and *spe-27* spermatids are swept from the gonad arm (*spe-8(hc50)*, *spe-8(hc50)* mated and *spe-27(it110)*). Thus, a block to spermiogenesis short circuits the sperm-sensing mechanism.

References

Hodgkin, J. and Barnes, T. M. (1991). More is not better: brood size and population growth in a self-fertilizing nematode. *Proc. R. Soc. Lond. B Biol. Sci.* **246**, 19-24.

Singson, A., Mercer, K. B. and L'Hernault, S. W. (1998). The *C. elegans spe-9* gene encodes a sperm transmembrane protein that contains EGF-like repeats and is required for fertilization. *Cell* **93**, 71-79.